Molecular Effects on the Opacity of the Vapor Created During Tokamak Disruptions: Formalism, Methods and Examples

R.R. Peterson and Wang Ping

May 1993

FPA-93-2

FUSION POWER ASSOCIATES

2 Professional Drive, Suite 248
Gaithersburg, Maryland 20879
(301) 258-0545

1500 Engineering Drive
Madison, Wisconsin 53706
(608) 263-2308

Molecular Effects on the Opacity of the Vapor Created During Tokamak Disruptions: Formalism, Methods and Examples

Robert R. Peterson and Wang Ping

Fusion Power Associates
402 Gammon Place
Suite 280
Madison, WI 53719

May 1993

FPA-93-2

1. Introduction

Radiation transport in the vapor created from wall or divertor material during a tokamak disruption is important to understanding the behavior of the vapor. Most of the energy in disruption ions during the thermal quench phase is deposited in already vaporized material and that energy will lead to additional vaporization only if it is transported to the unvaporized material in some way. It is believed [1] that radiation transport may be the main mechanism for this heat transfer. To accurately calculate the radiation transport, one needs to know the opacity of the vapor. If vapor is optically thin, the details of the opacity are not important because the emitted radiation will be transported approximately isotropically and will not be substantially re-absorbed by the vapor. However, the emissivity of the vapor, which is related to the opacity, will determine the rate that radiant energy is deposited in the unvaporized material. In the case of an optically thin vapor, roughly one-half of the radiation will reach the surface and vaporization of the material will likely continue. Once the vapor becomes optically thick, the details of the opacity become more important and the radiation transport may become non-isotropic. The opacity profile in an optically thick vapor will determine where the radiation diffuses. If the opacity of the vapor nearest the wall or divertor is higher than the opacity nearer the center of the tokamak, then radiation will primarily transport away from the unvaporized material and the wall or divertor will be self-shielded.

The issue of self-shielding is critical to the ITER concept. The fluence on the surface of the divertor during a disruption is thought to be in the range of 2000 to 6000 J/cm^2 [2,3]. The pulse is divided into two phases: the thermal quench is a pulse of 2000 to 3000 J/cm^2 over 0.1 to 3 ms while the current quench has about 3000 J/cm^2 in a pulse width of between 5 and 100 ms. If the radiation transport in the vapor is isotropic and if the thermal conduction in the divertor or wall can be neglected, 3000 J/cm^2 will vaporize 0.1 mm of graphite. This estimate made by assuming that all of the energy is converted into latent heat of vaporization. Since 500 disruptions are expected over the ten year lifetime of ITER, 5 mm would be eroded per year under such conditions. If, on the other hand, only 5% of the energy is radiated to the wall, 0.5 mm would be eroded in a year; 1% would lead to no more than 0.1 mm per year. To provide for adequate steady state heat transfer, the walls and divertors need to be as thin as possible. If 5 mm is removed each year, the divertors or walls would most likely have to be replaced at least yearly. Therefore, whether 50%, 5% or 1% of the energy deposited in the vapor is radiated to

the wall is important to the design of the walls and divertors on the operations and maintenance of ITER.

The calculation of the opacity of the vapor is therefore a very important element in the design and analysis of ITER. The standard opacity tables used in radiation hydrodynamic computer codes may not be valid for the conditions of the vapor. For example, there are reasons to suspect the validity of the SESAME tables [4,5] at low temperatures for some materials. At temperatures low enough to allow the existence of molecules, the vibrations and rotations of molecules will be important to the equation of state and opacity. Los Alamos National Laboratory has used the PANDA computer code [6] in some of the calculations of the SESAME tables, which does include rotations and vibrations, though it is sometimes unclear what molecular energy levels are included in the calculations for a given SESAME table. The molecular phenomena will be most important in the self-shielding calculations nearest the unvaporized material, where the vapor is the coldest and it is most important to accurately know the opacity. If the vaporizing material is graphite, it is well-known that the vapor may be leaving the surface as C_2, C_3, and C_4 [7]. Also, any impurities in the graphite or plasma will participate in the vapor chemistry.

There exist several examples where molecular effects in vapors and gases play important roles in radiation transport at the temperatures expected in disruption vapors. In a disruption on a graphite divertor plate, the vapor temperature will typically range from the sublimation temperature of graphite, about 0.4 eV, to about 5 eV. The radiative behavior of air during an atmospheric atomic explosion has been known for many years to depend strongly on molecular effects [8,9]. In such blasts, there are many mechanisms by which photons are emitted and absorbed, including photoionization of atoms and molecules and molecular absorption by excitation of rotational or vibrational states in several molecular species. Molecules of oxygen and nitrogen are present in the air below about 1.5 eV and photoionization of these molecules dominates the radiative properties from about 0.8 eV to 1.5 eV. In the air temperature range of 0.6 to 0.8 eV, absorption of photons produced in the blast is dominated by "photoionization of NO molecules, absorption by negative oxygen ions and molecular absorption by O_2, N_2, and NO molecules" [9]. Below about 0.5 eV, NO_2 is the dominant absorber.

Examples of low temperature plasmas where molecular effects are important are common in the technology of processing materials with plasmas. One application of considerable interest is the use of silane (SiH_4) plasmas to create thin films of silicon. In

some recently published work [10], a 0.5 eV, low density cascaded arc plasma jet is created from a mixture of argon, silane and hydrogen gases. Emission spectroscopy is used to measure the plasma temperature in this system. There is enough SiH present to make rotational and vibrational transitions a usable source of emitted radiation for temperature diagnostics. This diagnostic technique has been used also in plasmas containing CH [11].

To calculate the molecular contribution to the opacity one needs to first calculate the populations of molecular species and then calculate the radiative properties for each species present. We will present a formalism for calculating the chemical rate and equilibrium coefficients needed to solve the time-dependent and time-independent chemical reaction problems that determine the populations of molecular species. The CHEMKIN set of computer codes has been developed at Sandia National Laboratories [12] and is based on some of the formalism presented here. CHEMKIN includes a substantial database of thermodynamic properties that are useful in calculating chemical equilibrium and rate coefficients. Still, there are data needs that CHEMKIN cannot provide. Methods for calculating unknown data are suggested. An estimate of the equilibrium coefficients is made for reactions that convert atomic carbon into several polyatomic species. Opacities, including molecular effects, can be calculated once the molecular species are known. Methods for calculating photon absorption in diatomic molecules are discussed. The formalism is then used to estimate the absorption by diatomic carbon. This is then compared with a calculation of absorption by atomic carbon done with the IONMIX computer code [13].

2. Chemical Kinetics

2.1. Formalism

It is necessary to determine the concentrations for the k^{th} of K molecules $[\chi_k]$ as a function of time and space. Each molecule can undergo I reactions to form other molecules, generally represented as:

$$\sum_{k=1}^{K} \nu_{ki}^{'} \chi_k \rightleftharpoons \sum_{k=1}^{K} \nu_{ki}^{''} \chi_k \,. \qquad (i = 1, ..., I) \tag{1}$$

The stoichiometric integers are $\nu_{ki.}$ The key quantity that needs to be determined is the net production rate for the k^{th} molecular species:

$$\dot{\omega}_k = \sum_{i=1}^{I} \nu_{ki} q_i \,. \qquad (k = 1, ..., K) \tag{2}$$

Here, $\nu_{ki} = \nu''_{ki} - \nu'_{ki}$. It is evident from equation 2 that the rate-of-process parameter q_i contains the important details for the reaction rates.

The rate-of-process is defined as the difference between the forward and reverse rates

$$q_i = k_{f_i} \prod_{k=1}^{K} [\chi_k]^{\nu'_{ki}} - k_{r_i} \prod_{k=1}^{K} [\chi_k]^{\nu''_{ki}} \ . \tag{3}$$

The forward and reverse rate constants for the i^{th} process are k_{f_i} and k_{r_i}, respectively. For molecular transformation processes, the forward rate constant can be calculated as:

$$k_{f_i} = A_i T^{\beta_i} \exp \frac{-E_i}{T} \tag{4}$$

where E_i is the activation energy for the process and T is the temperature. A_i and β_i are coefficients for the i^{th} process. For vibrational transitions, equation 4 is replaced by the Landau-Teller expression:

$$k_{f_i} = A_i T^{\beta_i} \exp \left(\frac{B_i}{T^{\frac{1}{3}}} + \frac{C_i}{T^{\frac{2}{3}}} \right) \tag{5}$$

The reverse rate constants can be calculated from the forward rate constants with the use of equilibrium constants

$$k_{r_i} = \frac{k_{f_i}}{K_{c_i}} \tag{6}$$

The equilibrium constant for the i^{th} process, K_{c_i}, is calculated from the thermodynamic properties of the gas.

The equilibrium constants have the temperature dependence expressed in the following relation:

$$K_{c_i} = K_{p_i} \left(\frac{P_{atm}}{RT} \right)^{\sum_{k=1}^{K} \nu_{ki}} \ . \tag{7}$$

Here, P_{atm} is 1 atmosphere of pressure and

$$K_{p_i} = \exp \left(\sum_{k=1}^{K} \nu_{ki} \frac{S^o_k}{R} - \sum_{k=1}^{K} \nu_{ki} \frac{H^o_k}{RT} \right) ; \tag{8}$$

S^o_k is the standard state entropy and H^o_k is the standard state enthalpy.

2.2. Chemical kinetic parameters

From the formalism presented in the preceding section, it is clear that the time-dependent concentrations can be calculated if certain parameters are known. The forward

rate constant is determined by either of equations 4 or 5. A_i and β_i and either E_i or B_i and C_i are required to calculate k_{f_i}. We have found no universal database where these are available for a wide range of reactions. When these are not available, the rate coefficients can be estimated in some cases.

For diatomic molecules, dissociation and recombination rates can be roughly estimated by assuming that each collision between atoms in the presence of a third body results in recombination. The recombination rate is estimated to be

$$k_{r_i} = \beta \bar{v} \sigma \frac{4}{3} \pi r^3 \ , \tag{9}$$

where β is the fraction of collisions resulting in recombination (assumed to be equal to 1 in this approximation), $\bar{v}$ is the mean thermal speed and σ is the collision cross section. r is the molecular radius. Interactions are assumed to occur only when the atoms are within the molecular radius of each other. For dissociation of a diatomic molecule, the colliding particles must have more energy than the dissociation energy. For Maxwellian velocity distributions, the number of collisions with energies greater than the dissociation energy, U, is the dissociation rate

$$k_{f_i} = PN \left(\frac{8kT}{\mu \pi} \right)^{1/2} \sigma \frac{1}{s!} \left(\frac{U}{kT} \right)^s e^{-U/kT} \ . \tag{10}$$

s is a number that characterizes the importance of vibrational and rotational degrees of freedom in competing for the collision energy and adds 1 for each vibrational degree and 1/2 for each rotational degree. μ is the collision reduced mass and N is the number density. P is a factor, sometimes called the steric factor, representing the probability of a collision with sufficient energy causing dissociation.

In the preceding discussion, the rate coefficients depend upon the factors β and P, which must be measured or calculated by some more detailed method. The method of activated complexes is more physical, though it still calls upon measured of calculated parameters. Consider the reaction $XY + WZ \rightarrow XW + YZ$. In the process of performing the reaction, the atoms form the intermediate state $XYWZ$, which is called an activated complex and exists for a very short time. The activated complex is temporary because it has a potential energy that is higher than either the reactants or products. As is shown in Fig. 1, this potential energy of the activated complex constitutes a barrier to the reaction and therefore determines the rate of the reaction. An endothermic reaction may have the final state of the products $XW + YZ$ at as high a potential energy as the

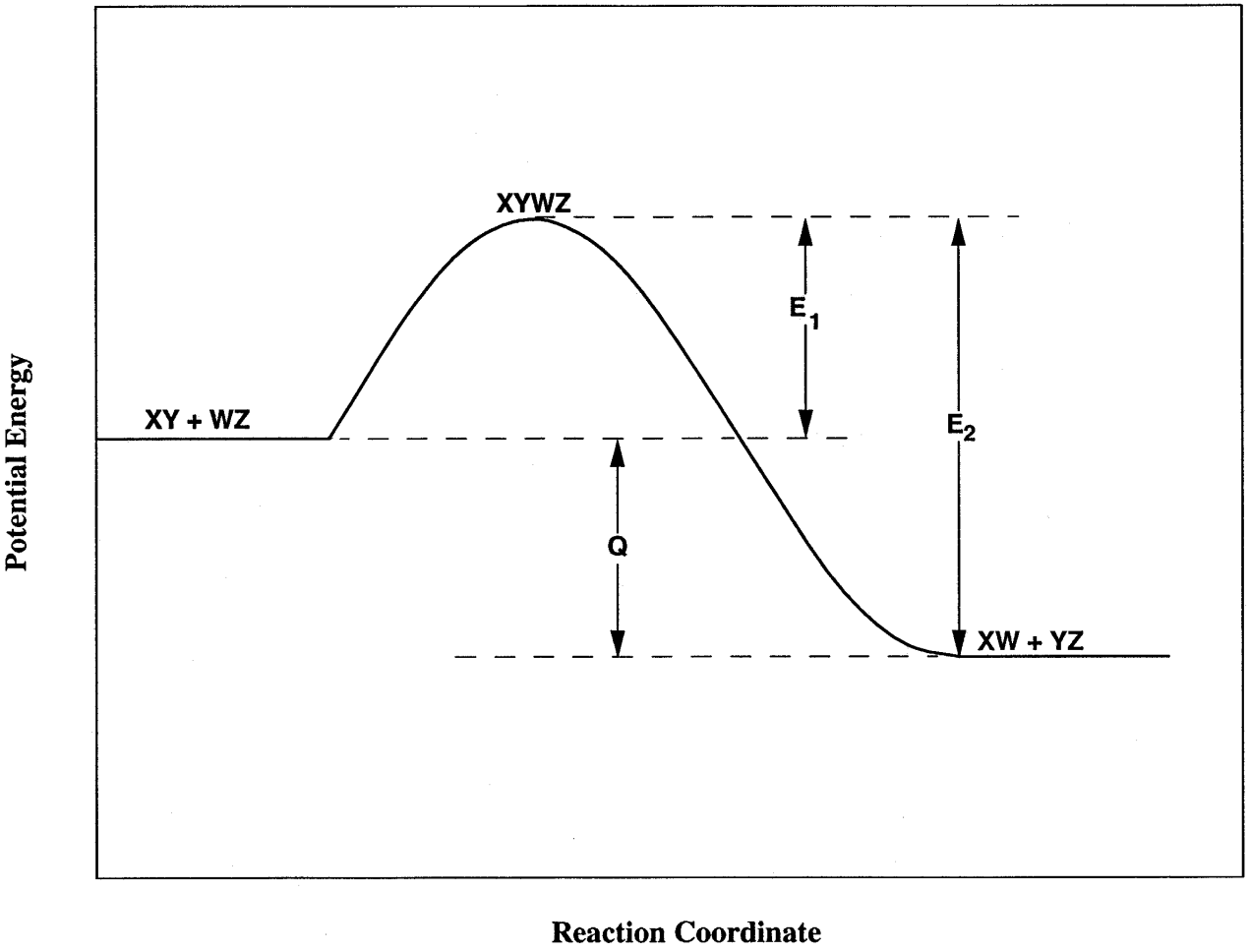

Figure 1. Activated complex potential barrier to chemical reactions.

activated complex and in this case that energy would determine the reaction rate. But all exothermic reactions have rates governed by the activated complex energy.

Using the concepts of collision theory discussed in the previous paragraph, the rate coefficient could be calculated from eqn. 10. The steric factor would still be an unknown parameter, which experimentally has been frequently measured to be quite small. A more definite calculation can be performed by considering all of the possible paths that the reaction can follow through molecular configuration space. Each path will have a different activation energy, E, to overcome and therefore a different rate. The most rapid paths will be those with the lowest activation energies. The activation energy is related to the linear dimensions of the activated complex, δ, which is roughly equal to the

molecular dimensions. The activated complex is unstable and remains a quasimolecule for a few ps. The rate coefficient can be calculated from the law of mass action with the ratio of partition functions for the activated complex, Z_{XYWZ}, to the reactants, Z_{XY} and Z_{WZ}[9]. Using this approach,

$$k_{f_i} = \frac{Z_{XYWZ}}{Z_{XY}Z_{WZ}} e^{-E/kT} \left(\frac{kT}{h^{1/2}} \right) . \tag{11}$$

Since the partition functions are all calculable, the steric factor can be deduced from this expression. The only remaining unknown parameter is E.

The equilibrium coefficients can be calculated from enthalpies and entropies that are available for many molecules. An example of an equilibrium coefficient calculation is shown in the next section.

2.3. Example Calculation for Carbon Vapor

As an example of a calculation, we have determined the equilibrium coefficients for carbon for temperatures that might be present in a tokamak disruption vapor. In the event that the vapor is in chemical equilibrium, the equilibrium coefficients will show which chemical species are most common in the vapor. We have chosen 5000 eV, 8000 eV and 11604 eV as temperatures of interest. Computer simulations with the CONRAD computer code have shown that the vapor on the surface of a tokamak divertor can reach temperatures of as high as 5 eV, though near the surface it is near the sublimation temperature of 4400 K.

For carbon vapor, one needs to consider the system of reactions:

$$\begin{array}{l} 2C \rightleftharpoons C_2 \\ 3C \rightleftharpoons C_3 \\ 4C \rightleftharpoons C_4 \\ 5C \rightleftharpoons C_5 \end{array} . \tag{12}$$

For these four reactions,

$$\nu_{ki}^{'} = \begin{pmatrix} 2 & 0 & 0 & 0 & 0 \\ 3 & 0 & 0 & 0 & 0 \\ 4 & 0 & 0 & 0 & 0 \\ 5 & 0 & 0 & 0 & 0 \end{pmatrix} \tag{13}$$

and

$$\nu''_{ki} = \begin{pmatrix} 0 & 1 & 0 & 0 & 0 \\ 0 & 0 & 1 & 0 & 0 \\ 0 & 0 & 0 & 1 & 0 \\ 0 & 0 & 0 & 0 & 1 \end{pmatrix}. \tag{14}$$

Since $\nu_{ki} = \nu''_{ki} - \nu'_{ki}$,

$$\nu_{ki} = \begin{pmatrix} -2 & 1 & 0 & 0 & 0 \\ -3 & 0 & 1 & 0 & 0 \\ -4 & 0 & 0 & 1 & 0 \\ -5 & 0 & 0 & 0 & 1 \end{pmatrix}. \tag{15}$$

The equilibrium coefficients are calculated from eqns. 7 and 8. The thermodynamic parameters H_k and S_k are recorded in the JANAF [14] tables and are stored in the CHEMKIN [12] computer code data base. The pertinent values for the reactions in eqn. 12 are shown in Table 1. With the information in Table 1 and the values for ν_{ki}, the equilibrium coefficients can be calculated. The four reactions of interest are given in Table 2. The temperature here was varied from 5000 K to 8000 K to 11604 K. The CHEMKIN database only reaches 5000 K, so we assumed that the S^o/R and H^o/R for all the temperatures are the same as at 5000 K. In Table 2, both the pressure equilibrium coefficients, K_p, and the concentration equilibrium coefficients, K_c, are shown. The equilibrium coefficients show that the thermodynamically favored species change as the temperature changes. At 5000 K, which is only 500 K above the boiling temperature of graphite [15], of the five species, C_5 is by far the most favored. At 8000 K, C_3 is the most favored, though there will be significant fractions of C, C_2, and C_4. At 1 eV, atomic carbon is the most significant species, though important amounts of C_2 and C_3 are present.

3. Radiative Absorption Coefficient of Diatomic Molecules

To study the molecular contributions to the opacity of the vapor near the divertor, it is natural to start from diatomic molecules.

Generally speaking, the procedures for calculating the molecular radiative absorption coefficient are basically the same as those for atoms. The basic information needed are the energy levels, radiative transition moments, and occupation probability of each level.

Table 1. Thermodynamic Properties for Molecular Carbon Species

Species	H°/R (K)	S°/R
C	106383	26.1
C_2	131769	36.0
C_3	127580	44.3
C_4	178285	53.1
C_5	240012	61.7

Table 2. Equilibrium Coefficients for Molecular Carbon Species

Reaction	K_p	K_c
T = 11604 K (1 eV)		
$C \rightleftharpoons C_2$	9.90×10^{-5}	0.094
$C \rightleftharpoons C_3$	2.56×10^{-8}	0.023
$C \rightleftharpoons C_4$	9.55×10^{-14}	8.25×10^{-5}
$C \rightleftharpoons C_5$	1.10×10^{-19}	9.04×10^{-8}
T = 8000 K (0.69 eV)		
$C \rightleftharpoons C_2$	2.24×10^{-3}	1.47
$C \rightleftharpoons C_3$	4.54×10^{-5}	19.5
$C \rightleftharpoons C_4$	1.38×10^{-9}	0.39
$C \rightleftharpoons C_5$	9.38×10^{-15}	1.77×10^{-3}
T = 5000 K (0.43 eV)		
$C \rightleftharpoons C_2$	1.0	410
$C \rightleftharpoons C_3$	1.66×10^{-2}	2.80×10^{3}
$C \rightleftharpoons C_4$	6.05	6.91×10^{7}
$C \rightleftharpoons C_5$	2.97×10^{4}	2.50×10^{19}

3.1. Energy Level Structure of Diatomic Molecules

The atomic nuclei in a molecule are held together by the electrons, since, according to the Coulomb law, the nuclei alone repel each other. The Coulomb and exchanged interactions of these charged particles (electrons and nuclei) produce the *electronic energies* E_e of the molecules. Just as for atoms, we shall expect different electronic states of the molecule, depending on the "*orbits*" in which electrons are. The different kinds of electronic states that have to be distinguished are designated by Σ, Π, Δ, $\cdots$, corresponding to the symbols S, P, D, $\cdots$ for atoms. The notation for a molecular state is given by

$$^{2S+1}\Lambda^{\pm}_{g,u}\,. \tag{16}$$

Here, S is the total spin of the system, $\Lambda = |M_L| = |\sum_i m_i|$ is the absolute value of the projected orbital angular momentum along the axis of the molecule, with $\Lambda = 0, 1, 2, \cdots$ designated by Σ, Π, Δ, and g, u, $+$, and $-$ are the indications of certain symmetries.

In each stable electronic state, the molecule can carry out vibrations about the equilibrium position, that is, can have a certain vibrational energy E_v. The molecule can also rotate, that is, have certain rotational energy E_r. Hence, the general picture for a molecule's level structure is that each electronic state has its own pattern of vibrational and rotational levels. To a very good approximation, the total energy E of the molecule is the sum of three component parts,

$$E = E_e + E_v + E_r\,. \tag{17}$$

For diatomic molecules, E_v and E_r can be expressed as

$$E_v = \omega_e(v+\frac{1}{2}) - \omega_e x_e(v+\frac{1}{2})^2 + \omega_e y_e(v+\frac{1}{2})^3 + \cdots, \tag{18}$$

and

$$E_r = B_v J(J+1) - D_v J^2(J+1)^2 + \cdots. \tag{19}$$

As an illustration, two different electronic states with their vibrational and rotational levels are represented graphically in Fig. 2. In orders of magnitude, molecular electronic states are separated by 10^4 to 10^5 cm^{-1} (visible, ultraviolet), vibrational levels are separated by 10^2 to 10^3 cm^{-1} (infrared), and rotational levels by 10^{-1} to 10^0 cm^{-1} (microwave).

A compilation of available energy data for all diatomic molecules and ions has been given by K.P. Huber and G. Herzberg [16] .

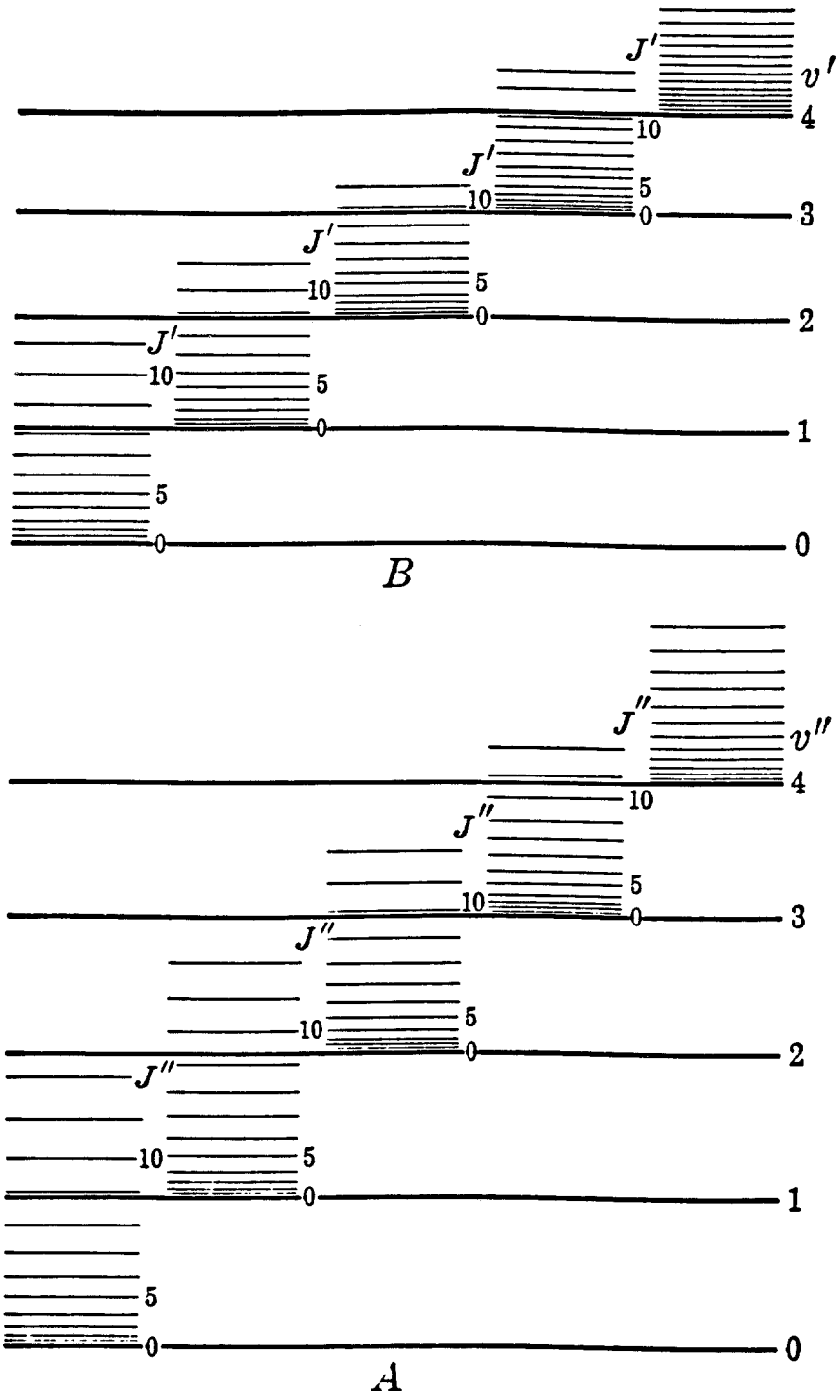

Figure 2. Vibrational and rotational states of two electronic states, A and B, of a molecule (schematic). Only the first few rotational and vibrational levels are drawn in each case.

3.2. Molecular Radiative Transition Moments

Consider an electronic transition between two nondegenerate levels or sub-levels, where a sub-level is one of the components of a degenerate electronic state. Just like the case for an atom, the absorption coefficient for such a transition between a lower state L and an upper state U is:

$$\mu(\nu) = N_L B_{L\to U} h\nu_{L\to U} F(\nu)\,, \tag{20}$$

where $\nu_{L\to U}$ is the line frequency, N_L is the particle density of the lower state, $B_{L\to U}$ is the Einstein coefficient for induced absorption, and $F(\nu)$ is a line shape factor such that

$$\int F(\nu)d\nu = 1\,. \tag{21}$$

By spectroscopic convention, the lower level is given by (n'', v'', J''), where n'' is the electronic state indicator, v'' is the vibrational quantum number, and J'' is the rotational quantum number. The upper level is then specified by (n', v', J'). Primes always refer to upper levels and double primes to lower levels. When ν is expressed in "wave number" (cm^{-1}), the Einstein coefficient for induced absorption is given by

$$B_{n'',v'',J'',n',v',J'} = \frac{8\pi^3}{3h^2c}\frac{\sum_{M'',M'}|R^{M'',M'}|^2}{2J''+1} \tag{22}$$

where

$$R^{M'',M'} = \int \psi''^{*}_{n'',v'',J'',M''}\mathbf{R}\psi'_{n',v',J',M'}d\tau \tag{23}$$

is the matrix element of the electronic moment operator $\mathbf{R} = \mathbf{R}_e + \mathbf{R}_n$ of the electrons an nuclei. Here M'' and M' are azimuthal quantum numbers numbering the spatially degenerate rotational levels of the lower and upper states, and the summation is over all possible combinations of the rotational sub-levels of the lower with those of the upper state.

By using the Born-Oppenheimer approximation [17], the molecular wave function may be written as a product

$$\psi = \psi_e\psi_{vib}\psi_{rot} \tag{24}$$

of the electronic, vibrational, and rotational wavefunctions. Hence we can have

$$\sum_{M'',M'}|R^{M'',M'}|^2 = |R_e|^2 q(v', v'')S_{J''} \tag{25}$$

where

$$|R_e|^2 = |\int \psi''^{*}_e\mathbf{R}_e\psi''_e d\tau_e|^2 \tag{26}$$

and

$$q(v', v'') = |\int \psi''_{vib}\psi'_{vib}dR|^2 \,. \tag{27}$$

The integration in eqn. 27 is over the internuclear separation. The R_e is the electronic transition moment, and $q(v', v'')$ is the Franck-Condon factor. The S_J is called the Honl-London intensity factor; it is that part of $\sum_{M'',M'} |R^{M'',M'}|^2$ that depends on the rotational quantum number J and the coupling in the molecule. It has been proved that S_J follows the sum rule[18]:

$$\sum_{J''} \frac{S_{J''}}{2J''+1} = 1 \,. \tag{28}$$

The Einstein coefficient for induced absorption can now be written as:

$$B_{n'',v'',J'',n',v',J'} = \frac{8\pi^3}{3h^2c}|R_e|^2 q(v', v'')\frac{S_{J''}}{2J''+1} \,. \tag{29}$$

For band averaged absorption, we have

$$B_{n'',v'',n',v'} = \frac{8\pi^3}{3h^2c}|R_e|^2 q(v', v'') \,. \tag{30}$$

As in the case for atoms, it is convenient to use the oscillator strength to describe the strength of radiative transitions. The oscillator strength for a particular molecular transition $(n'', v'', J'') \rightarrow (n', v', J')$ is defined as:

$$f_i = \frac{8\pi^2 mc}{3he^2}\frac{\nu_i}{g_{n''}}|R_e|^2 q(v', v'')\frac{S_{J''}}{2J''+1} \,. \tag{31}$$

The band absorption oscillator strength is:

$$f_{v'',v'} = \frac{8\pi^2 mc}{3he^2}\frac{\nu_{v'v''}}{g_{n''}}|R_e|^2 q(v', v'') \,, \tag{32}$$

while the averaged absorption oscillator strength, f_e, applicable to the entire electronic band system, is defined by:

$$f_{n'',n'} = \frac{8\pi^2 mc}{3he^2}\frac{\nu_{n'n''}}{g_{n''}}|R_e|^2 \,. \tag{33}$$

3.3. Level Occupation Probability

By assuming local thermodynamic equilibrium for the plasma, the occupation probability of a specified level (n', v', J') is given by

$$F_{n',v',J'} = \frac{(2J''+1)\omega_I}{Q_{tot}} \exp(-E_{n',v',J'}/kT) \tag{34}$$

where $E_{n',v',J'}$ is the energy of the level and ω_I is the nuclear spin statistical weight. Q_{tot} is the total partition function and may be written as the sum of contributions from all the electronic states:

$$Q_{tot} = \sum_n Q_n \,. \tag{35}$$

Taking into account electronic (orbital + spin), vibrational, rotational, and nuclear (spin only) degrees of freedom, we may write

$$Q_n = Q_{electronic} Q_{vib-rot} Q_{nuclear} \tag{36}$$

where

$$Q_{electronic} = \omega_\Lambda (2S+1) \exp(\frac{-hc\nu_{00}}{kT}) \,, \tag{37}$$

is the electronic partition function. S is the total electron spin, ω_Λ is the statistical weight for orbital angular momentum Λ about the internuclear axis and takes the value 1 if $\Lambda = 0$ and the value 2 if $\Lambda \neq 0$, and ν_{00} is the energy of the lowest vibrational level of the electronic state n above that of the ground state.

$$Q_{vib-rot} = \sum_{v=0}^{\infty} \exp[-\frac{hc}{kT}(E_v - E_0)] Q^v_{rot} \tag{38}$$

is the vibrational and rotational partition function. The pure rotational partition function is

$$Q^v_{rot} = \sum_{J=0}^{\infty} (2J+1) \exp[-\frac{hc}{kT} F_v(J)] \simeq \frac{KT}{hcB_v} \,. \tag{39}$$

The partition function for nuclear spin is

$$Q_{nuclear} = \frac{(2I_a+1)(2I_b+1)}{\sigma} \,. \tag{40}$$

I_a and I_b are the nuclear spins of the two nuclei and σ is a symmetry number having the value 2 for homonuclear molecules and 1 for heteronuclear systems.

An appropriate formula for $Q_{vib-rot}$ that is more convenient for calculation has been developed by Bethe[19]:

$$Q_{vib-rot} = \frac{1}{[1 - \exp(-1.4388\omega_0/T)]} \frac{T}{1.4388 B_0} (1 + \gamma T) \tag{41}$$

with

$$\gamma = \frac{1}{1.4388\omega_0} (\frac{2\omega_0 x_0}{\omega_0} + \frac{\alpha_0}{B_0} + \frac{8B_0}{\omega_0}) \,. \tag{42}$$

3.4. Radiative Absorption Coefficient

The radiative absorption coefficient at a particular wave number in an electronic band system of a diatomic gas is obtained by summation over all rotational lines of the individual line absorption coefficients evaluated at that wave number. The result depends on the band structure, the line shape and the influence of the various broadening mechanisms. The number of rotational lines within a vibrational band is so large that in most cases the width of each line is larger than the separation distance of two neighboring lines. Hence each vibrational band is well covered by lines. In large scale engineering calculations, the molecular radiative absorption coefficients are usually calculated by a method which uses a local average model for the rotational structure such that the absorption coefficient is continuous throughout each band. This method has been described by Keck et al. [20,21,22].

The radiative absorption coefficient in an electronic band system of a diatomic gas yielded by this procedure is calculated from the following expressions:

$$\mu_\nu = \frac{\pi e^2}{mc^2} g_{n''} f_e \frac{[N]}{Q_e} \frac{hc}{kT} \exp[-\frac{hc}{kT}(E'_0 - \nu)] \phi_\nu \tag{43}$$

and

$$\phi_\nu = \frac{kT/hc}{Q_v Q_r |B'_e - B''_e|} \sum_{v'v''} q_{v'v''} \exp\{-\frac{hc}{kT}[(E'_{v'} - E'_0) + \frac{B''_e}{|B'_e - B''_e|}(\nu - \nu_{v'v''})]\} . \tag{44}$$

In these expressions, μ_ν is in cm^{-1}, $[N]$ is the total number of molecules per cm^3, Q_e, Q_v and Q_r are the electronic, vibrational and rotational partition functions. $\nu_{v'v''}$ is the wave number for the vibrational transition between states v' and v''. $q_{v'v''}$ is the Franck-Condon factor of the (v', v'') band, and f_e is the electronic band averaged absorption oscillator strength. The temperature T is in the units of °K.

3.5. Absorption Coefficients of Phillips Bands And Swan Bands of C_2 Gas

By using the formulas discussed above, we have done a sample calculation for the radiative absorption coefficients of the Phillips bands ($A^1\Pi_u - X^1\Sigma_g^+$) and Swan bands ($d^3\Pi_g - a^3\Pi_u$) of C_2 gas. The related basic molecular constants were taken from Ref. 16 and listed in Table 3. The Franck-Condon factors were obtained from the table given by R.J. Spindler [23]. The results of the absorption coefficient calculations are shown in Fig. 3 for a temperature of 1 eV and a normalization concentration of 1 molecule per cm^3. Also shown in the figure are the absorption coefficients from IONMIX [13] for a C plasma

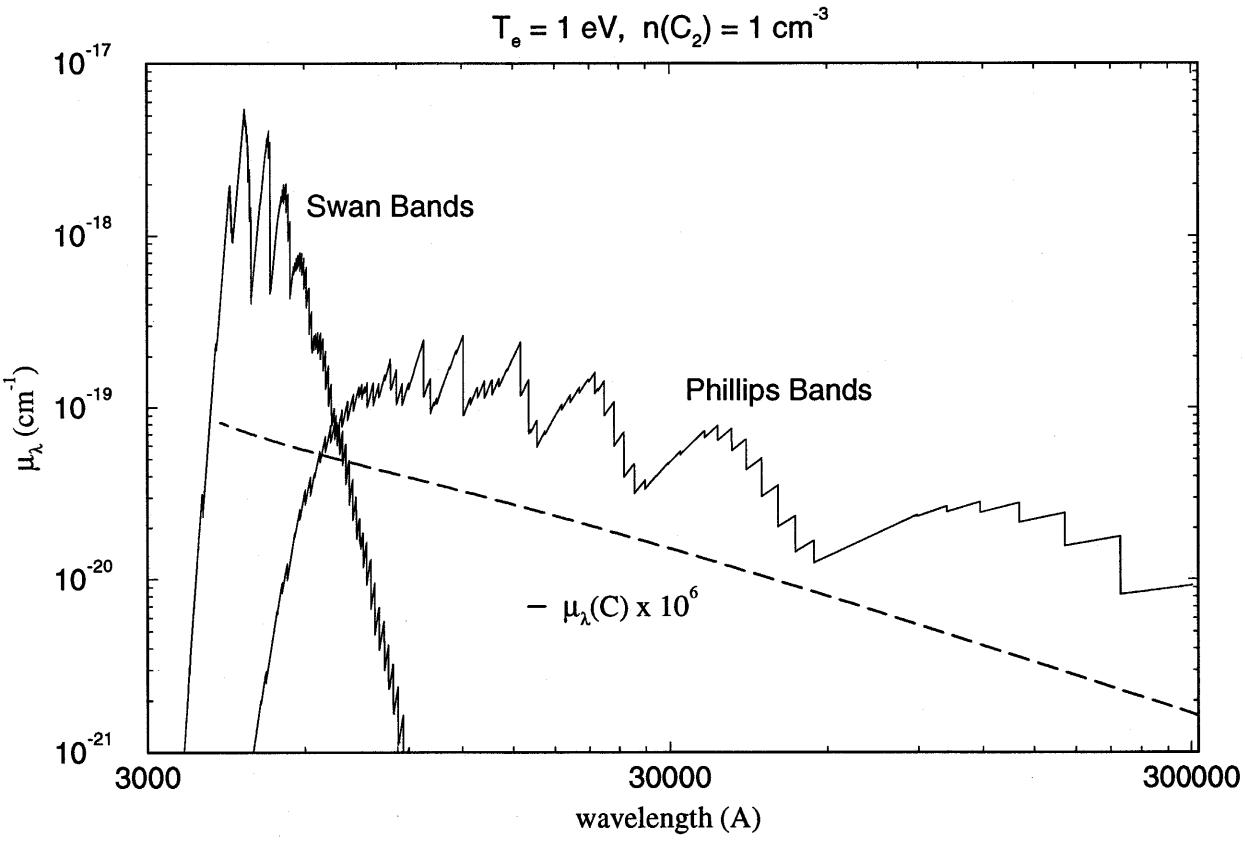

Figure 3. Radiation absorption coefficients of C_2.

without including molecular effects. It is seen that Swan bands are the major absorption bands. The curves have a "sawtooth" character, with each new tooth appearing when a new vibrational band is included in the absorption process. The absorption coefficients of atoms are much smaller than those of molecules.

4. Summary and Discussion

We have summarized methods for calculating populations of molecular species and radiative absorption in diatomic gases. We have used these methods to calculate chemical equilibrium coefficients for carbon vapor and absorption coefficients for diatomic and monatomic carbon. We believe that this lays the groundwork for the development

Table 3. Spectroscopic Constants for Molecular States of Phillips and Swan Bands of C_2

State	$E_e(\text{cm}^{-1})$	ω_e	$\omega_e x_e$	$\omega_e y_e$	B_e	α_e	D_e	Transitions
d $^3\Pi_g$	20022.50	1788.22	16.44	-0.5067	1.7527	0.01608	6.74	Swan bands: $d \leftrightarrow a$
A $^1\Pi_u$	8391.00	1608.35	12.07	-0.010	1.6163	0.01686	6.44	$\nu_{00} = 19378.44$ $f_e = 0.020$
a $^3\Pi_u$	716.24	1641.35	11.67	—	1.6324	0.01661	6.44	Phillips bands: $A \leftrightarrow X$
X $^1\Sigma_g^+$	0.00	18.54.71	13.34	-0.172	1.8198	0.01765	6.91	$\nu_{00} = 8268.16$ $f_e = 0.0025$

of computer codes to calculate the equation of state and optical properties of molecular vapors and gases.

The examples we have performed for carbon show that molecular effects are important to tokamak disruption vapors. Computer simulations [24] have shown that the vapor blown off of a divertor plate during a disruption will be at a few eV. The surface of the graphite coated divertor will be no hotter than the sublimation temperature of 4100 C, so some of the vapor will be in the 1 eV range. Our estimates have shown that a 1 eV carbon vapor will be about 90% monatomic and 10% diatomic. We have also shown that the absorption of photons below about 4 eV by diatomic molecules is six orders of magnitude higher than in monatomic carbon. Therefore, the effect of diatomic molecules under these conditions is five orders of magnitude more than the monatomic atoms. The absorption coefficient at a wavelength of 1.2 microns (1 eV) is about 10^{-19} cm^{-1} for 1 atom per cm^3 or, at the typical density of 5×10^{17} cm^{-3}, the absorption length is 20 cm. The vapor is 10's of cm thick, so molecular effects make the vapor marginally optically thick. Without molecular effects, the vapor is clearly optically thin.

Acknowledgement

Support for the work has been provided by Kernforschungszentrum Karlsruhe, through Fusion Power Associates.

References

1. R.R. Peterson, "Radiation Transport in Self-Protecting Vapor in Tokamak First Walls During Disruptions," Bull. Amer. Phys. Soc. **27**, 1130 (1982).

2. "ITER Plasma Facing Components," ITER Documentation Series, No. **30**, IAEA, (1991).

3. R.T. McGrath, A.J. Russo, R.B. Campbell, and R.D. Watson, "Plasma Facing Component Development: Boundary Layer Physics and Component Engineering," Fusion Technology **21**, 1805 (1992).

4. "T-4 Handbook of Material Properties Data Bases," Los Alamos National Laboratory Report LA-10160-MS (November 1984), ed. K.S. Holian.

5. R.R. Peterson, et al., "Inertial Confinement Fusion Reactor Cavity Analysis: Progress Report for the Period 1 July 1986 to 30 June 1987," University of Wisconsin Fusion Technology Institute Report UWFDM-725 (July 1987).

6. G.I. Kerley, "Users Manual for PANDA: A Computer Code for Calculating Equations of State," Los Alamos National Laboratory Report LA-8833-M (November 1981).

7. A.J.C. Ladd, "Condensation of Ablated First-Wall Materials in the CASCADE Inertial Confinement Fusion Reactor," Lawrence Livermore National Laboratory Report UCRL-53697 (Dec. 1985).

8. U.S. Dept. of Defense, *The Effects of Nuclear Weapons*, McGraw-Hill, New York, (1950).

9. Ya. B. Zel'dovich and Yu. P. Raizer, *Physics of Shock Waves and High-Temperature Hydrodynamic Phenomena*, Academic Press, New York, (1966)

10. G.J. Meeusen, et al., "Emission Spectroscopy on a Supersonically Expanding Argon/Silane Plasma," J. Appl. Phys. **71**, 4156 (1992).

11. J. Koulidiati, et al., Colloq. Phys. C5, **51**, 297 (1990).

12. R.J. Kee, et al., "A Fortran Computer Code Package for the Evaluation of Gas-Phase Multicomponent Transport Properties," Sandia National Laboratories Report SAND86-8246 (1986).

13. J.J. MacFarlane, "IONMIX-A Code for Computing the Equation of State and Radiative Properties of LTE and Non-LTE Plasmas," University of Wisconsin Fusion Technology Institute Report UWFDM-750 (1987).

14. JANAF Thermochemical Tables, Natl. Stand. Ref. Data Ser. NSRDS-NBS 37, (1971).

15. *Handbook of Chemistry and Physics*, 48th College Edition, The Chemical Rubber Company, Cleveland, OH (1968).

16. K.P. Huber and G. Herzberg, *Molecular Spectra And Molecular Structure. IV. Constants of Diatomic Molecules*, Van Nostrand (1979).

17. M. Weissbluth, *Atoms And Molecules*, Academic Press, New York (1978).

18. G. Herzberg, *Spectra of Diatomic Molecules*, pp. 208, 2nd ed., D. Van Nostrand, New York, (1950).

19. H.A. Bethe, *The Specific Heat of Air Up to 25,000°C*, OSRD Report 369 (1942).

20. J.C. Keck, et al., Ann. Phys. **7**, 1 (1959).

21. J.C. Keck, et al., JQSRT **3**, 335 (1963).

22. R.W. Patch, et al., JQSRT **2**, 263 (1961).

23. R.J. Spindler, JQSRT **5**, 165 (1965).

24. R.R. Peterson, "Computer Modeling of Self-Shielding Vapor During Tokamak Disruptions," Bull. APS **37**, 1600 (1992).